VOLUME 5, NUMBER 9, SEPTEMBER 2005

NANO LETTERS

DNA Translocation in Inorganic Nanotubes

Rong Fan,[†] Rohit Karnik,[‡] Min Yue,[‡] Deyu Li,[‡] Arun Majumdar,*[,‡,§] and Peidong Yang*[,†,§]

Department of Chemistry, University of California, Berkeley, California 94720, Department of Mechanical Engineering, University of California, Berkeley, California 94720, and Materials Sciences Division, Lawrence Berkeley National Laboratory, Berkeley, California 94720

Received May 23, 2005; Revised Manuscript Received June 14, 2005

ABSTRACT

Inorganic nanotubes were successfully integrated with microfluidic systems to create nanofluidic devices for single DNA molecule sensing. Inorganic nanotubes are unique in their high aspect ratio and exhibit translocation characteristics in which the DNA is fully stretched. Transient changes of ionic current indicate DNA translocation events. A transition from current decrease to current enhancement during translocation was observed on changing the buffer concentration, suggesting interplay between electrostatic charge and geometric blockage effects. These inorganic nanotube nanofluidic devices represent a new platform for the study of single biomolecule translocation with the potential for integration into nanofluidic circuits.

The detection of individual biomolecules has been realized in nanofluidic devices and shows potential applications ranging from single molecule study of biological activity to rapid diagnosis of diseases.[1] Biological nanochannels/pores, e.g., α-hemolysin, were first used over a decade ago to detect single-stranded polynucleotides and show great promise for ultrafast DNA sequencing.[2−4] Recently, artificial inorganic nanopores are attracting increasing attention due to the robustness of solid-state nanopore membranes, the flexibility of surface modification, and the precise control of nanopore sizes.[5−8] The artificial nanopores have been used to study analytes ranging from small molecules, single-stranded polynucleotides, to double-stranded DNAs (dsDNAs). The molecular translocation can be probed from ionic current signals. In addition, nanotubule membranes have been used to sense DNAs with single base mismatch selectivity.[9]

Inorganic nanotubes, which represent a new class of one-dimensional nanostuctures, are attracting increasing attention.[10] Inspired by nanopore technology, we use chemically synthesized inorganic nanotubes as the core elements and integrate them with microfluidic systems for single-molecule sensing. Compared with traditional nanopore devices, these nanotube devices feature three distinct differences. First, these nanotubes (∼10 μm long) have very high aspect ratio such that they can confine the entire biomolecule, which is likely to result in new translocation characteristics. Second, our devices have a planar layout, which could enable

* Corresponding authors. E-mail: p_yang@berkeley.edu; majumdar@me.berkeley.edu.
[†] Department of Chemistry, University of California, Berkeley.
[‡] Department of Mechanical Engineering, University of California, Berkeley.
[§] Materials Sciences Division, Lawrence Berkeley National Laboratory.

10.1021/nl0509677 CCC: $30.25
Published on Web 06/28/2005

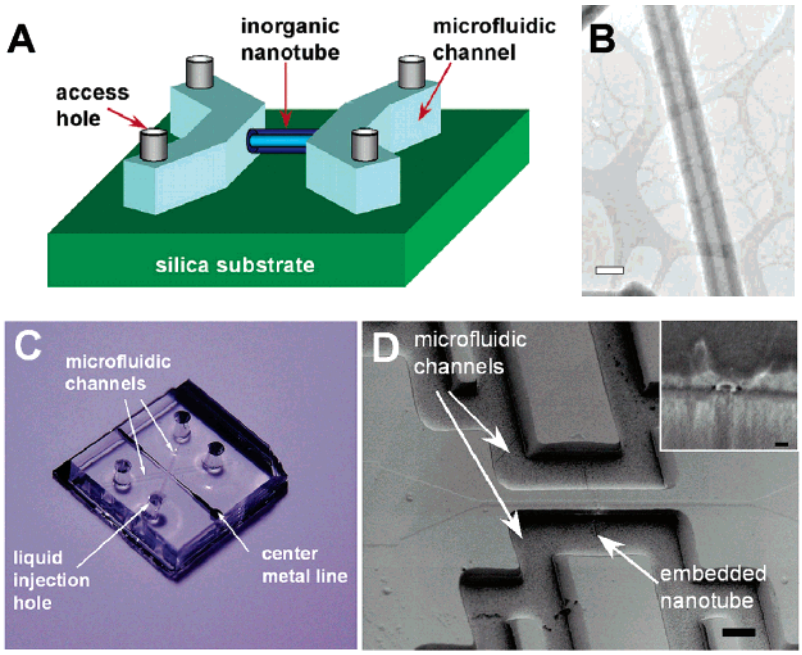

Figure 1. Inorganic nanotube nanofluidic devices. (A) Schematic of device structure features a single nanotube bridging two microfluidic channels to form a nanofluidic system. (B) Representative transmission electron micrograph of the chemically synthesized silica nanotube. Scale bar represents 100 nm. Typical nanotubes in the experiments are ~50 nm in inner diameter. (C) A fully packaged nanofluidic device. (D) Scanning electron micrograph of the nanofluidic device before cover bonding. Scale bar represents 10 μm. Inset shows cross-section view of the nanotube embedded between two silicon dioxide layers. Scale bar represents 100 nm.

simultaneous optical and electrical probing. Third, the current device geometry is compatible and amenable to integration with lab-on-a-chip micro-total-analysis systems (μTASs), and microelectronics. Moreover, the advance of self-assembly techniques, such as Langmuir−Blodgett assembly,[11] provides convenient routes for fabricating large-scale arrays of nanofluidic devices for parallel processing.

Figure 1A is the schematic of a nanotube nanofluidic device that features a single inorganic nanotube bridging two microfluidic channels. Uniform silicon nanowires synthesized by $SiCl_4$ chemical vapor deposition were translated into silica nanotubes through an oxidation/etching process with controlled wall thickness and pore size down to 10 nm as shown in Figure 1B.[12] Nanotubes used in the present study had an inner diameter of typically 50 nm. A fully packaged nanofluidic device with microfluidic channels and inlet/outlet ports is shown in Figure 1C. A scanning electron micrograph (Figure 1D) further shows the integration of a single nanotube with microfluidic channels. The cross-sectional view (inset) clearly shows the opening of the nanotube embedded between two silicon dioxide layers.

In our experiment, both microfluidic channels were filled with 2 M potassium chloride (KCl) buffer solution,[13] and ionic current was recorded with an applied voltage bias (Figure 2A). No transient current change was observed although the baseline shifted slightly over time. When λ-DNA molecules in 2 M KCl buffer were introduced into the negatively biased microchannel while the other microchannel was filled only with buffer, the ionic current exhibited frequent drops in current corresponding to the passage of λ-DNAs through the nanotube (Figure 2B). These current drop events may be attributed to the geometrical exclusion effect of conducting ions because of the finite size of λ-DNA, leading to transient ionic current blockage. Although, the noise level is relatively high, these ionic current drops can still be resolved and were highly reproducible. Statistics of current drop and duration are shown in Figure 1C. The typical current change was 10−40 pA; the typical duration was 4−10 ms with a small fraction of events up to 20 ms. The overall distribution was quite narrow and centered around 23 pA and 7.5 ms, suggesting that most of the events were identical, corresponding to single molecule translocation. Furthermore, once the polarity of the applied bias was reversed, no signal peaks were observed which reveals the DNA translocation was electrophoretically driven. For electrically charged particles in aqueous solution, the electrophoretic mobility is approximately $\mu_{EP} = q/6\pi\eta r$ (q the charge of particles, η the viscosity, r the particle size). This relationship applies to spherical particles and is a rough approximation. Since the persistence length of double-stranded DNA is about 50 nm (ref 14), it is likely that the DNA molecules are fully stretched in the nanotube with a diameter of 50 nm. The particle size r can be approximated by the end-to-end distance of the stretched DNA molecule. The end-to-end distance L_z, estimated using the de Gennes dynamics model,[15] is about 5.8 μm. Experimental study of stretching λ-DNA in nanochannels gave an average L_z about 8 μm (ref 16). This means that the entire λ-DNA molecule could stay inside the nanotube during translocation. The electrophoretic mobility of λ-DNA in the nanotube is calculated to be $\sim 1 \times 10^{-8}$ m^2/(V s) and the resulting DNA transport velocity is ~2 μm/ms under bias of 1 V. Consequently, the predicted translocation duration is 2.5 ms, which is in agreement with the shortest limit of observed events.

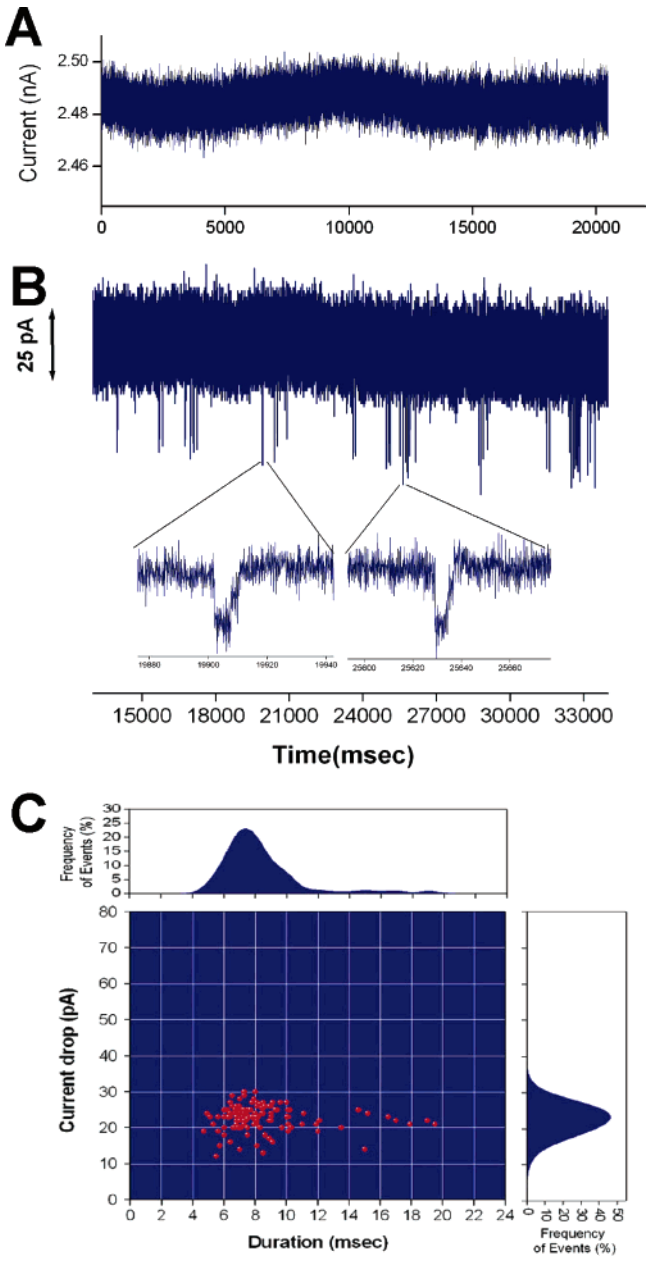

Figure 2. Ionic current signals for λ-DNA translocations with 2 M KCl buffer. (A) Control experiment with 2 M KCl buffer solutions in both microchannels. (B) Typical ionic current signal recorded when a λ-DNA ($\sim$30 μg/mL) test solution (prepared with 2 M KCl buffer) was loaded to the negatively biased (0.4 V) microchannel, showing extensive current drop spikes. Current drop signals were not observed when the bias polarity was reversed. (C) Statistics of current drop and duration time for three measurements. The main plot shows the pattern of all events, with a tight distribution indicating single molecule translocation scheme. The top and right insets are the event frequency as a function of duration time and current drop, respectively.

Due to the interactions of biomolecules with the surface electric double layer, it is reasonable to expect a longer translocation time. Moreover, electroosmotic flow could add an opposite force to slow the translocation of DNA molecules.

Interestingly, when the same experiment was conducted using lower concentrations of KCl (0.5 M) buffer solution, a distinctly different phenomenon was observed. Instead of current decrease, frequent current increases were observed

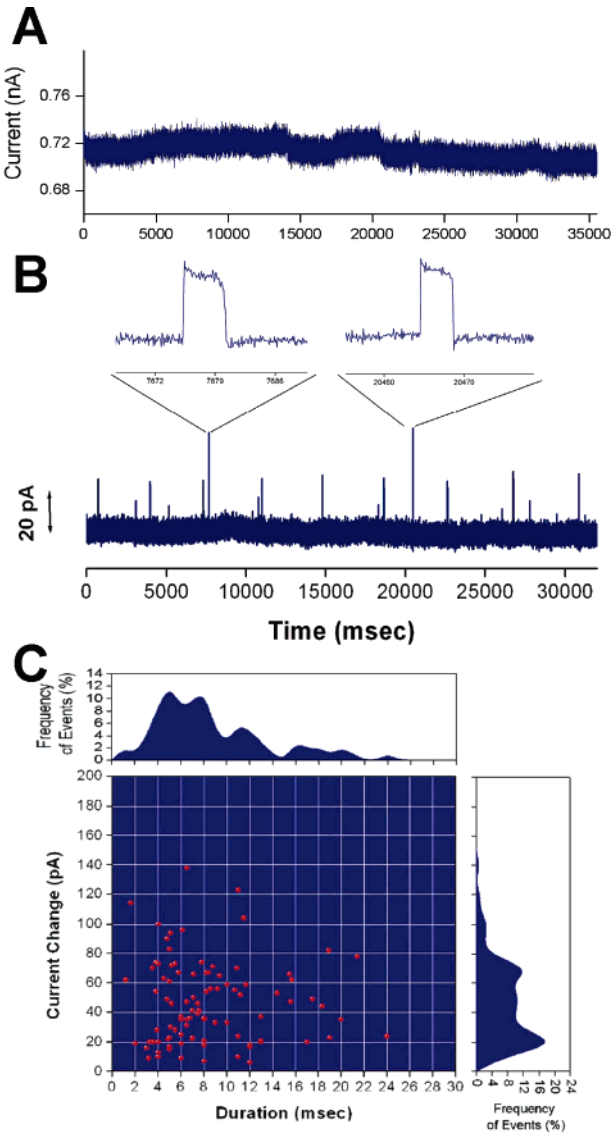

Figure 3. Ionic current signals for λ-DNA translocations with 0.5 M KCl buffer. (A) Control experiment with 0.5 M KCl buffer solutions in both microchannels. (B) Typical ionic current signal recorded when a λ-DNA ($\sim$6 μg/mL) test solution (prepared with 0.5 M KCl buffer) was loaded to the negatively biased (1 V) microchannel. Unexpectedly, extensive current increase spikes were observed rather than current drops. This was not observed when the bias polarity was reversed. (C) Statistics of current drop and duration time for four measurements. The main plot shows the pattern of all events showing a relatively broader distribution. The top and right insets are the event frequency as a function of duration time and current drop, respectively.

corresponding to the passage of λ-DNA molecules (Figure 3B). The control experiment exhibited some baseline shifts, although no abrupt current changes were observed (Figure 3A). The translocation characteristics were different compared with the 2 M KCl case—statistics of current change and duration time showed a much broader distribution. This is the first observation of ionic current crossover, i.e., a transition from current blockage to current enhancement during DNA translocation through nanotubes as a result of their unique dimensions. Ionic current increase during DNA translocation through 50−60 nm long nanotubes was previously observed by Chang et al.[17] The current enhancement

was attributed to the introduction of counterions in the nanotube due to the charge on DNA molecules dominating over the steric blockage effect observed in other studies. Our experiments confirm their observations and further elucidate that there is a crossover from current enhancement to current blockage that depends on ionic concentration.

When DNA molecules enter the nanotube, the number of cations and anions in the nanotubes would decrease due to the volume exclusion effect. At the same time, DNA molecules also carry counterions (cations) into the nanotube, which may transiently increase the cation concentration. Here we build on the arguments presented by Chang et al.,[17] and develop a simple model. Assuming that Manning condensation[18] of counterions neutralizes a fraction $(1 - \phi)$ of the negative phosphate groups of DNA leaving fraction ϕ for mobile counterions to interact with, the change Δn in the mobile counterion density inside the nanotube is

$$\Delta n = \Delta n_{\mathrm{CHARGE}} + \Delta n_{\mathrm{BLOCK}} = \frac{2\phi b}{N_{\mathrm{A}} V_{\mathrm{nt}}} - \frac{V_{\mathrm{mol}}(n_+ + n_-)}{V_{\mathrm{nt}}} \quad (1)$$

where b is the number of base pairs (48500 for λ-DNA), V_{nt} is the volume of the nanotube, V_{mol} is the volume occupied by the DNA molecule, n_+ and n_- are the cation and anion densities, respectively, within the nanotube in the absence of DNA, and N_{A} is the Avogadro's number. The first term ($\Delta n_{\mathrm{CHARGE}}$) corresponds to the increase in mobile counterion concentration due to the presence of DNA (i.e., the molecular gating effect), whereas the second term ($\Delta n_{\mathrm{BLOCK}}$) is the steric exclusion of both cations and anions. We note here that the expression for $\Delta n_{\mathrm{CHARGE}}$ is only approximately given by eq 1. In our experiments, KCl was used as the electrolyte. The ionic mobilities for K^+ and Cl^- are $\mu_{K^+} \sim 7.62 \times 10^{-8}$ m^2/(V s) and $\mu_{Cl^-} \sim 7.91 \times 10^{-8}$ m^2/(V s), respectively. So the current change during DNA molecule translocation is

$$\Delta I = \Delta I_{\mathrm{CHARGE}} - \Delta I_{\mathrm{BLOCK}} = \left\{ \Delta n_{\mathrm{CHARGE}} \mu_{K^+} - \left(\frac{\Delta n_{\mathrm{BLOCK}}}{2} \right) [\mu_{K^+} + \mu_{Cl^-}] \right\} e N_{\mathrm{A}} A E \quad (2)$$

where A is the cross sectional area of the nanotube, E is the magnitude of the electric field across the nanotube, and $\Delta I_{\mathrm{CHARGE}}$ and $\Delta I_{\mathrm{BLOCK}}$ denote the current changes corresponding to the charge effect and the steric blockade effect, respectively.[19]

Equations 1 and 2 suggest that there exists a critical ion concentration, n_{cr}, such that $\Delta I > 0$ when $\Delta I_{\mathrm{CHARGE}} > \Delta I_{\mathrm{BLOCK}}$ and $\Delta I < 0$ when $\Delta I_{\mathrm{CHARGE}} < \Delta I_{\mathrm{BLOCK}}$ as illustrated in Figure 4. The critical total ion concentration is given as

$$n_{\mathrm{cr}} = \frac{4\phi b}{V_{\mathrm{mol}} N_{\mathrm{A}}} \left(\frac{\mu_{K^+}}{\mu_{K^+} + \mu_{Cl^-}} \right) \quad (3)$$

and the critical KCl concentration is $C_{\mathrm{cr}} = n_{\mathrm{cr}}/2$. Note that for a linear molecule such as DNA, $V_{\mathrm{mol}} = \pi r^2 p b$, where r is the radius of the double helix and p is the length per base pair (=0.34 nm). For dsDNA molecules, ϕ ranges from 0.17 to 0.5 based on previous reports and simulation.[20,21] Here it is assumed that $\phi = 0.5$ for Manning condensation, and $r =$ 1 nm. Therefore, the critical KCl concentration is estimated as $n_{\mathrm{cr}} \sim 0.79$ M.

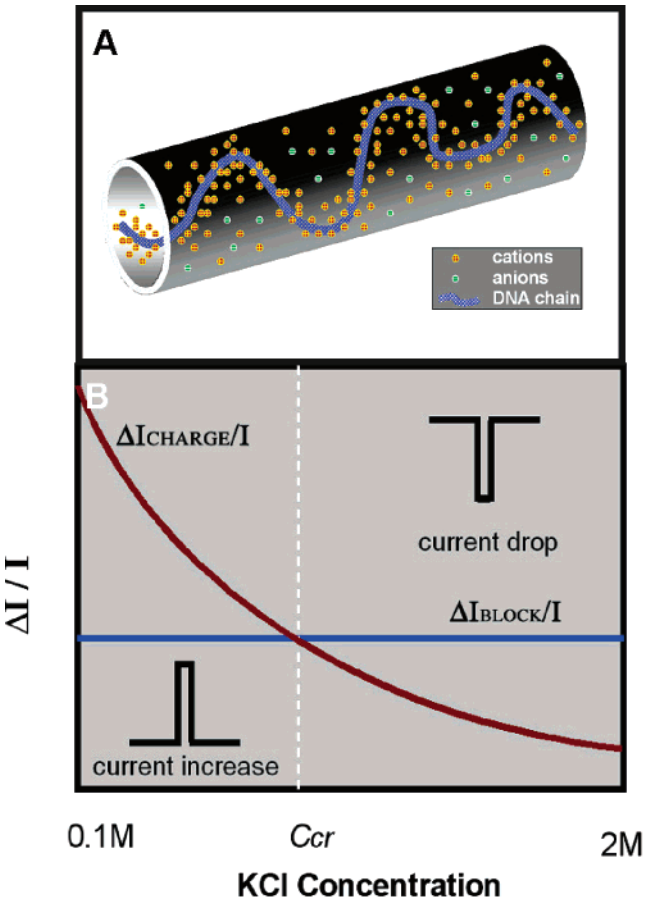

Figure 4. (A) Schematic illustration of ionic distribution of counterions and co-ions in an inorganic nanotube when DNA molecule is confined inside. (B) Schematic illustration showing the interplay of charge effect and blockade effect.

This simple scheme indicates there is an ionic current crossover (from current blockade to current enhancement) for DNA translocation through a nanotube as the KCl concentration is decreased below the critical concentration (~0.79 M). This has been indeed observed in our experiments. Equation 2 predicts a net current blockade of 20 pA for 2 M KCl, which again agrees very well with the experimental data (~20−30 pA). The predicted current increase for 0.5 M KCl is 6 pA, which corresponds to the lowest limit in our observation. Our model assumes that during translocation, the ionic environment of the DNA molecule corresponds to the bulk electrolyte composition. The Debye length (<1 nm) under experimental conditions is much smaller than the nanotube diameter (~50 nm) and DNA is not expected to adsorb on the negatively charged oxide nanotube walls. Under these conditions our assumption is valid and the oxide charge would not significantly affect our results, which is corroborated by the agreement between the observed critical concentration and that predicted by eq 3. While this scheme qualitatively explains our experimental observation, we would like to point out that this is perhaps an oversimplified account of the highly complex DNA transport process within nanotubes filled with electrolytes.

Our inorganic nanotube nanofluidic device extends the single molecule transport events greatly in time scale compared to the nanopore devices. In addition, the duration, the current change, the current decay characteristics measured at different ionic concentrations, and bias could provide useful information on biomolecules within a confined geometry. Therefore, these nanotube devices represent a new platform for studying single molecule behavior. We are working on an experimental setup for simultaneous optical and electrical probing that would provide independent evidence of DNA translocation through the nanotubes and potentially yield new insights into these translocation events. Due to their planar design and compatibility with standard microfabrication technology, this basic module of inorganic nanotube nanofluidics could be further integrated into nanofluidic circuits for high throughput and parallel analysis of biological species at the single molecule level.

Acknowledgment. This work was supported by the IMAT program, National Cancer Institute, and the Basic Energy Sciences, Department of Energy. We also thank Richard Cote, Ram Datar, Hirofumi Daiguji, and Andrew Szeri for their collaboration. A.M. would like to thank the Miller Institute for a Professorship. P.Y. is an A. P. Sloan Fellow. We thank the Microfabrication Laboratory (UC Berkeley) and the National Center for Electron Microscopy for the use of their facilities.

Supporting Information Available: Descriptions of the fabrication of nanotube nanofluidic devices and electrical measurements. This material is available free of charge via the Internet at http://pubs.acs.org.

References

(1) Turner, S. W. P.; Cabodi, M.; Craighead, H. G. *Phys. Rev. Lett.* **2002**, *88*, 128103.
(2) Kasianowicz, J. J.; Brandin, E.; Branton, D.; Deamer, D. W. *Proc. Natl. Acad. Sci. U.S.A.* **1996**, *93*, 13770.
(3) Deamer, D. W.; Akeson, M. *Trends Biotechnol.* **2000**, *18*, 147.
(4) Howorka, S.; Cheley, S.; Bayley, H. *Nature Biotechnol.* **2001**, *19*, 636.
(5) Li, J.; Stein, D.; McMullan, C.; Branton, D.; Aziz, M. J.; Golovchenko, J. A. *Nature* **2001**, *412*, 166.
(6) Storm, A. J.; Chen, J. H.; Ling, X. S.; Zandbergen, H. W.; Dekker, C. *Nat. Mater.* **2003**, *2*, 537.
(7) Saleh, O. A.; Sohn, L. L. *Nano Lett.* **2003**, *3*, 37.
(8) Siwy, Z.; Trofin, L.; Kohli, P.; Baker, L.; Trautmann, C.; Martin, C. R. *J. Am. Chem. Soc.* **2005**, *127*, 5000.
(9) Kohli, P.; Harrell, C. C.; Cao, Z. H.; Gasparac, R.; Tan, W. H.; Martin, C. R. *Science* **2004**, *305*, 984.
(10) Goldberger, J.; He, R. R.; Zhang, Y. F.; Lee, S. W.; Yan, H. Q.; Choi, H. J.; Yang, P. D. *Nature* **2003**, *422*, 599.
(11) Tao, A.; Kim, F.; Hess, C.; Goldberger, J.; He, R. R.; Sun, Y. G.; Xia, Y. N.; Yang, P. D. *Nano Lett.* **2003**, *3*, 1229.
(12) Fan, R.; Wu, Y.; Li, D.; Yue, M.; Majumdar, A.; Yang P. D. *J. Am. Chem. Soc.* **2003**, *125*, 5254.
(13) All the test solutions in our experiment were prepared with DNA buffer solution, which consists of 10 mM NaCl, 10 mM Tris-HCl, and 1 mM EDTA in aqueous solution. pH = 7.6.
(14) Smith, S. B.; Cui, Y.; Bustamante, C. *Science* **1996**, *271*, 795.
(15) De Gennes, P. G. *Scaling concept in polymer physics*; Cornell University Press: Ithaca, NY, 1979.
(16) Tegenfedt, J. O.; Prinz, C.; Cao, H.; Chou, S.; Reisner, W. W.; Riehn, R.; Wang, Y. M.; Cox, E. C.; Sturm, J. C.; Silbersan, P.; Austin, R. *Proc. Natl. Acad. Sci. U.S.A.* **2004**, *101*, 10979.
(17) Chang, H.; Kosari, F.; Andreadakis, G.; Alam, M. A.; Vasmatzis, G.; Bashir, R. *Nano. Lett.* **2004**, *4*, 1551.
(18) Manning, G. *Biophys. Chem.* **2002**, *101*, 461.
(19) Current carried by a translocating biomolecule itself is negligible compared to ionic current due to low biomolecular mobility.
(20) Padmanabhan, S.; Richey, B.; Anderson, C. F.; Record, J. M. T. *Biochemistry* **1988**, *27*, 4367.
(21) Ravishanker, G.; Aunger, P.; Langley, D. R.; Jayaram, B.; Young, M. A.; Beveridge, D. L. *Rev. Comput. Chem.* **1997**, *11*, 317.

NL0509677